

# Adversarial Water-Filling: Theory, Algorithms and Foundation Model

Xindi Tong, Chee Wei Tan, H. Vincent Poor

**Abstract**—Competitive resource allocation problems over frequency and space can be formulated as minimax interaction between transmit power and worst-case interference. This formulation naturally arises in multi-operator low Earth orbit (LEO) satellite spectrum sharing, where transmissions from competing constellations interfere in real-time. Under Gaussian channels, AWF is strongly convex–concave on nondegenerate active channels, whereas discrete constellations yield generally nonconvex mercury/water-filling formulations. In this paper we propose the Adversarial Water-Filling (AWF) problem with corresponding theory and algorithms for these real situations. In addition, we develop a wireless foundation model for AWF to learn the AWF search dynamics. The architecture incorporates permutation-invariant channel representations, a constraint-aware graph neural network (GNN) with sparse message passing, and global latent variables capturing the low-dimensional water level implied by the AWF optimality. Through learned projected extragradient iterations, the model approximates stationary solutions of the constrained minimax problem arising under mercury/water-filling. We further show that, under local regularity and contractivity conditions, the learned AWF dynamics converge locally linearly around regular stationary points. Experiments demonstrate empirical generalization across unseen problem sizes, different constraints, and multiple discrete constellations, while achieving more than one-order-of-magnitude runtime improvements over iterative baselines. The related code can be found at <https://github.com/convexsoft/AWF>.

**Index Terms**—Adversarial water-filling, minimax optimization, wireless foundation models, spectrum sharing.

## I. INTRODUCTION

The sixth generation (6G) mobile communication network is envisioned to be AI-native, where intelligence is embedded throughout network design, operation, and service provisioning [1]. This requires scalable and autonomous resource adaptation as a key system principle [2]. Within this paradigm, Open RAN has emerged as a transformative architecture enabling multi-vendor interoperability through standardized open interfaces [3]. Such architectural flexibility becomes particularly important as next-generation networks integrate high-altitude platform stations and non-terrestrial networks (NTNs) to support large-scale low Earth orbit (LEO) constellations [4]–[6]. Recent LEO direct-to-device proceedings involving Starlink and Omnispace have raised reported coexistence concerns, highlighting competitive interference and spectrum-coordination challenges under mobility, beam dynamics, directional links, and overlapping spectrum use [7].

Unlike traditional cellular systems with relatively fixed base-station deployments, NTN coexistence creates a space-time varying interference environment. A representative exam-

## Multi-Operator LEO Competition under Shared Spectrum

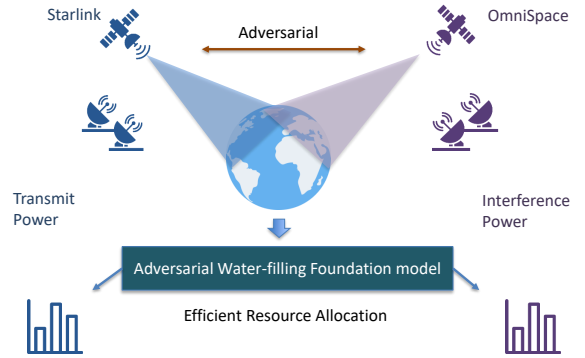


Fig. 1. Competition between Starlink and Omnispace gives rise to a minimax resource-allocation problem, for which the AWF foundation model provides an efficient solution.

ple is the emerging coexistence between Starlink direct-to-cell services and Omnispace-like mobile-satellite systems under shared or adjacent spectrum and regulatory constraints [7]. Highly directional beams, overlapping footprints, heterogeneous antenna gains, and terrestrial–satellite spectrum reuse make interference strongly location dependent, while satellite motion, beam steering, short visibility windows, and handovers continuously reshape the dominant interferers and coupling strengths [8]. Consequently, one operator’s transmission may appear as uncertain and rapidly changing interference to another operator, motivating adversarial resource allocation robust to worst-case space–time interference (cf. Fig. 1). Existing studies on multi-operator NTN coexistence show that power flux density limits, equivalent isotropically radiated power masks, orbital geometry, beam directivity, frequency reuse, and payload flexibility strongly affect interference footprints and coexistence performance [9]–[12]. These observations motivate an optimization framework that models spatial coupling, temporal variation, and competitive interference interactions.

From an information-theoretic perspective, water-filling provides the fundamental mechanism for power allocation over parallel Gaussian channels [13]. For practical discrete constellations, the mercury/water-filling extends this principle by incorporating modulation-dependent “mercury levels” through the I–MMSE relationship [14]. While Gaussian water-filling yields concave problems with well-characterized solutions, mercury/water-filling introduces more intricate utility curvature and may lose global convex–concave properties under adversarial interference. This motivates a minimax formulation for competitive NTN spectrum sharing. Recent work further connects water-filling with modern optimization by interpreting it as a proximal operator parameterized by a small number of dual variables [15]. Under spatial constraints and multi-

Xindi Tong and Chee Wei Tan are with the College of Computing and Data Science (CCDS), Nanyang Technological University, Singapore. H. Vincent Poor is the Michael Henry Strater University Professor in Princeton University, United States E-mail: to0002di@e.ntu.edu.sg, cheewei.tan@ntu.edu.sg, poor@princeton.edu

operator competition [16], [17], these water levels become dual variables linking high-dimensional channel allocations. This viewpoint connects AWF to primal–dual optimization methods such as the primal–dual hybrid gradient (PDHG) algorithm [18], [19], as well as distributed multi-agent optimization frameworks studied in game-theoretic processing [20]. However, most model-based methods typically need to be executed from scratch for each new network instance and do not naturally generalize across varying channel dimensions, constraint types, or modulation distributions.

Learning-based approaches have therefore been explored to accelerate wireless resource allocation [21]. Although these methods can reduce computational latency, most existing approaches remain task-specific and dimension-dependent, limiting their adaptability to heterogeneous and rapidly evolving 6G environments. More recently, the concept of wireless foundation models has emerged as a promising paradigm for capturing invariances that generalize across tasks and system configurations [22]. Rather than replacing model-based optimization, foundation models aim to encode physical symmetries and coupling structures in a transferable manner, enabling the model to learn solution strategies that transfer across related optimization problems.

In this paper, we introduce adversarial water-filling (AWF) as a unified framework for competitive wireless resource allocation over frequency and space, covering adversarial Gaussian water-filling and mercury/water-filling in competitive NTN spectrum sharing. AWF naturally supports a foundation-model approach through channel permutation invariance, sparse constraint-induced interactions, and global water-level coordination via dual variables. Inspired by classical Gaussian water-filling [15] and primal–dual/proximal methods [18], [19], we develop a domain-specific wireless foundation model with permutation-invariant channel representations, constraint-graph propagation, and learned primal–dual dynamics. The same pre-trained model is reused without instance-specific re-training across channel dimensions, constraint patterns, and modulation formats, enabling zero-shot transfer across AWF resource-allocation tasks. A preliminary conference version appeared in [23], focusing on Gaussian AWF in Open RAN, proximal/PDHG interpretation, and finite-step water-level search. This journal version substantially extends it to spatially constrained and mercury/water-filling AWF, with new foundation-model architecture, Karush–Kuhn–Tucker (KKT)/local-convergence analysis, and cross-size, cross-constraint, and cross-modulation generalization experiments. The main contributions of this paper are summarized as follows:

- We formulate an adversarial water-filling minimax framework for multi-operator LEO satellite spectrum sharing, explicitly modeling worst-case interference interactions under spatial constraints.
- We unify Gaussian water-filling and mercury/water-filling within a common minimax formulation and identify both convex–concave regimes and more challenging nonconvex regimes.
- We propose a foundation model based on a primal–dual architecture that combines permutation-invariant set

encoding, graph neural message passing over constraints, and learned primal–dual updates for water-level optimization, and implement it on an NVIDIA GPU for experimental evaluation.

- We establish theoretical properties including conditional KKT consistency and local convergence under regularity and contractivity conditions, and demonstrate empirical generalization across problem sizes, constraint types, and modulation distributions representative of large-scale LEO deployments.

## II. RELATED WORK

### A. Water-Filling and Minimax Games

Water-filling is a fundamental principle for information-theoretic power allocation, originating from optimal resource allocation over parallel Gaussian channels [24]. It has been widely applied to SISO, OFDM, and MIMO systems [25]. For practical discrete constellations, mercury/water-filling introduces modulation-dependent corrections through the I–MMSE relationship, thereby extending classical results beyond Gaussian signaling [14]. Iterative water-filling algorithms have also been extensively studied for Gaussian multiuser channels and are known to converge to optimal or equilibrium power allocations under suitable conditions [26]. This naturally leads to a game-theoretic interpretation: in multiuser interference channels, each transmitter performs water-filling against the interference generated by other users, while the coupled sum-rate maximization problem is generally nonconvex [27].

When interference is no longer a fixed impairment but an uncertain and potentially adversarial action, power allocation can be formulated as a two-player minimax problem. Such minimax formulations have been extensively studied in convex optimization and game theory, with classical results establishing the existence of saddle points and efficient methods for computing equilibria [28]. However, most existing water-filling formulations assume known channel statistics and predictable interference levels, which limits their applicability to competitive NTN environments where interference may be uncertain, nonstationary, and operator dependent.

First-order methods, including PDHG and related proximal algorithms, provide practical tools for solving large-scale instances of such problems [18], [19]. Worst-case and max–min formulations have appeared in anti-jamming communications, where transmit strategies are designed to maintain throughput under uncertain or malicious interference [29]. Related multi-access game models further examine interactions between selfish users and adaptive jammers under Nash or Stackelberg formulations [30].

Despite these advances, existing game-theoretic and water-filling methods are often derived for fixed problem dimensions, known uncertainty sets, or Gaussian signaling assumptions. They do not readily accommodate the combination of spatially coupled constraints, non-Gaussian mercury/water-filling utilities, and unpredictable multi-operator interference in NTN spectrum sharing. Building on these foundations, the present work formulates AWF as a minimax game that explicitly characterizes worst-case interference while extending water-filling to spatial constraints and practical non-Gaussian signaling.

### B. Learning-Based Spectrum Management

Learning has been widely explored to accelerate wireless resource allocation under complex and dynamic network conditions. Early work used neural networks to approximate optimization solution mappings for fast inference [21], later extending to dynamic settings via continual and bilevel optimization [31]. Reinforcement learning and multi-agent methods have been applied to distributed power control and spectrum sharing [32], while graph neural networks can exploit wireless channel graphs to capture interference coupling and improve scalability in resource allocation [33]. Model-based deep learning can improve interpretability and robustness by embedding iterative optimization principles into neural architectures [34]. However, unpredictable NTN coexistence introduces additional challenges beyond conventional learning-based spectrum management. The number of visible satellites, active beams, dominant interferers, constraint patterns, and modulation formats may change across time, space, and operators. As a result, models trained for a fixed topology or a fixed channel dimension may fail to generalize under distribution shifts caused by satellite mobility, beam steering, handovers, and adversarial interference. Permutation-invariant architectures, such as Deep Sets, Set Transformer, and Perceiver, provide useful tools for size-generalized modeling of unordered channel sets [35]–[37], while graph-based representations can encode spatial coupling induced by interference and regulatory constraints.

More recently, wireless foundation models and knowledge-driven deep learning have been explored for large-scale 6G optimization, emphasizing transferability, large-scale pretraining, and domain-structured inductive bias [22]. NVIDIA has also advanced this direction through OpenRAN Gym on platforms for advanced wireless research (PAWR) infrastructures, enabling large-scale data collection and learning-based experimentation for multi-operator scenarios [38]. PAWR provides programmable wireless testbeds for validating new communication techniques and network architectures under realistic conditions, bridging simulation and real-world evaluation for learning-based spectrum management. These developments suggest that a foundation model for spectrum management should go beyond approximating an algorithm and instead learn the dynamics of optimization under uncertain, size-varying, and unpredictable interference conditions. This motivates our constraint-varying and size-generalized AWF foundation model for competitive NTN resource allocation.

### III. ADVERSARIAL WATER-FILLING OVER FREQUENCY

We consider a resource allocation problem with a global budget constraint, where the objective is separable across components but coupling arises through the total resource constraint. Water-filling characterizes this structure by equalizing marginal utilities across all active components. In conventional settings with fixed receiver noise, this leads to optimal power-allocation strategies for parallel Gaussian channels [39]. We extend this framework to an AWF problem in which the receiver faces variable interference subject to a global interference budget. The resulting formulation naturally leads

to a minimax resource-allocation problem between transmit power and adversarial interference, reminiscent of worst-case power control and spectrum allocation in wireless networks over frequency [28], [40].

Consider  $m$  channels with transmit power  $p \in \mathbb{R}_{\geq 0}^m$  and interference power  $n \in \mathbb{R}_{\geq 0}^m$ . Channel  $i$  has channel gain  $\beta_i > 0$  and background noise  $\sigma_i > 0$ . Both players satisfy global budgets  $\mathbf{1}^\top p = P$  and  $\mathbf{1}^\top n = N$ . The AWF problem over frequency is formulated as

$$\max_{p \geq 0, \mathbf{1}^\top p = P} \min_{n \geq 0, \mathbf{1}^\top n = N} f(p, n), \quad (1)$$

where  $f(p, n)$  depends on the modulation model.

#### A. Gaussian Water-filling

For Gaussian channels, the achievable sum capacity (in nats per channel use) is

$$f(p, n) = \sum_{i=1}^m \log \left( 1 + \frac{\beta_i p_i}{\sigma_i + n_i} \right). \quad (2)$$

For fixed  $n$ ,  $f(p, n)$  is strongly concave in  $p$  over the feasible simplex, while for fixed  $p$  with  $p_i > 0$ ,  $f(p, n)$  is convex in the corresponding interference variables  $n_i$  due to  $\sigma_i > 0$ . Over the feasible set, the Gaussian AWF exhibits a strongly convex–concave game, which guarantees the existence and uniqueness of the minimax solution. The resulting problem is formulated as the following constrained max–min optimization:

$$\max_{p \geq 0} \min_{n \geq 0} \sum_{i=1}^m \log \left( 1 + \frac{\beta_i p_i}{\sigma_i + n_i} \right), \quad (3)$$

subject to  $\mathbf{1}^\top p = P$  and  $\mathbf{1}^\top n = N$ .

*Optimal Power Allocation.* For a fixed interference vector  $n$ , the maximization over  $p$  reduces to the water-filling problem. The optimal transmit power allocation takes the form

$$p_i^* = \max \left( \nu - \frac{\sigma_i + n_i^*}{\beta_i}, 0 \right), \quad \forall i \quad (4)$$

where  $\nu$  is the water level determined by the power constraint.

Conversely, for a fixed transmit power allocation  $p$ , the adversarial interference allocation minimizing the capacity is obtained via the corresponding Lagrangian formulation, leading to the closed-form expression

$$n_i^* = \max \left( -\frac{\beta_i p_i^*}{2} + \frac{1}{2} \sqrt{(\beta_i p_i^*)^2 - 4 \frac{\beta_i p_i^*}{\mu} - \sigma_i}, 0 \right), \quad \forall i \quad (5)$$

where  $\mu$  is the dual variable associated with the total interference power constraint  $\mathbf{1}^\top n = N$  [28]. The minimax formulation of the water-filling problem reveals a strong alignment between active transmit and interference channels, as formalized in the following result.

**Theorem 1** (Adversarial Water-filling over Frequency). *Consider the minimax problem in (3). Let  $(p^*, n^*)$  denote an optimal solution.*

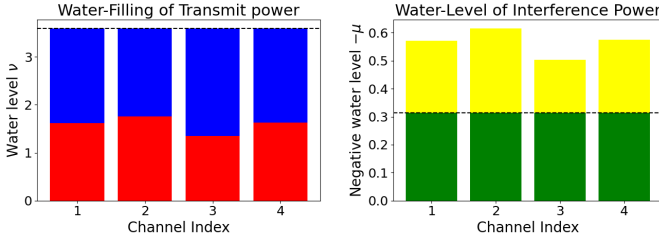


Fig. 2. Illustration of adversarial water-filling. (a) Transmit-side water-filling for  $p^*$ , where the dashed line denotes the water level  $\nu$ , red bars denote effective base levels  $(\sigma + n^*)/\beta$ , and blue segments denote powers  $p^*$ . (b) Interference allocation for  $n^*$ , where the dashed line denotes the interference water level  $-\mu$ , the total bar height is  $1/(\sigma + n^*)$ , and yellow segments denote  $1/(\beta\nu)$ .

- Inactive channels: For any  $i \in \{1, \dots, m\}$ , if  $p_i^* = 0$ , then the corresponding interference allocation satisfies  $n_i^* = 0$ .
- Active channels: For any  $i \in \{1, \dots, m\}$  with  $p_i^* > 0$  and  $n_i^* > 0$ , the interference dual variable  $\mu$  satisfies  $\mu = \frac{1}{\beta_i \nu} - \frac{1}{\sigma_i + n_i^*}$ .

*Proof.* If  $p_i^* = 0$ , substituting into the closed-form expression (5) gives  $n_i^* = 0$  since  $\sigma_i > 0$ . Hence channels inactive for transmission also receive zero interference allocation [23].

For channels with  $p_i^* > 0$ , consider the interference minimization subproblem with fixed  $p^*$ . The Lagrangian is

$$\mathcal{L}(n, \mu, c) = \sum_{i=1}^m \log \left( 1 + \frac{\beta_i p_i^*}{\sigma_i + n_i} \right) + \mu(N - \mathbf{1}^\top n) - c^\top n, \quad (6)$$

where  $\mu$  and  $c \geq 0$  are the dual variables. For any channel  $i$  with  $n_i^* > 0$ , complementary slackness gives  $c_i = 0$ , and the stationarity condition yields

$$-\frac{\beta_i p_i^*}{(\sigma_i + n_i^*)(\sigma_i + n_i^* + \beta_i p_i^*)} - \mu = 0. \quad (7)$$

Substituting the transmit water-filling solution (4) into the above equation leads to  $\mu = \frac{1}{\beta_i \nu} - \frac{1}{\sigma_i + n_i^*}$  for any  $i \in \{1, \dots, m\}$  with  $p_i^* > 0$ .  $\square$

The above relation shows that the adversarial interference allocation induces a water level  $\mu$  coupled with the transmit-side water level  $\nu$ . This problem therefore yields dual water levels for both transmit power and interference power, as illustrated in Fig. 2.

### B. Mercury/water-filling

We keep the same variables and constraints  $(p, n, P, N, \beta_i, \sigma_i)$ , but replace the logarithmic utility by a mutual-information objective induced by an input distribution that could be mercury:

$$f(p, n) = \sum_{i=1}^m I_i \left( \frac{\beta_i p_i}{\sigma_i + n_i} \right), \quad \text{s.t.} \quad \gamma_i = \frac{\beta_i p_i}{\sigma_i + n_i}. \quad (8)$$

Here  $I_i(\gamma)$  denotes the mutual information (in nats/use) of channel  $i$  as a function of the SINR  $\gamma$ . For Gaussian inputs,

$I_i(\gamma) = \log(1 + \gamma)$  and the model reduces to the Gaussian-channel case. The minimax game becomes

$$\max_{p \geq 0, \mathbf{1}^\top p = P} \min_{n \geq 0, \mathbf{1}^\top n = N} \sum_{i=1}^m I_i(\gamma_i). \quad (9)$$

Theorem 1 can be naturally extended to the mercury/water-filling problem over frequency. For fixed interference power  $n$ , the transmit-power optimality condition for any active channel  $i \in \{1, \dots, m\}$  with  $p_i^* > 0$  is

$$\frac{\beta_i}{\sigma_i + n_i^*} I'_i(\gamma_i^*) = \nu, \quad (10)$$

where  $\nu$  enforces  $\mathbf{1}^\top p = P$ . The interference-power optimality condition for any  $i \in \{1, \dots, m\}$  with  $n_i^* > 0$  is

$$-\frac{\beta_i p_i^*}{(\sigma_i + n_i^*)^2} I'_i(\gamma_i^*) = \mu, \quad (11)$$

where  $\mu$  enforces  $\mathbf{1}^\top n = N$ . Using the I-MMSE identity [41],

$$I'_i(\gamma) = \text{mmse}_i(\gamma), \quad \forall i \quad (12)$$

(10)–(11) define a dual water-filling system, with transmit-side and interference-side water levels  $\nu$  and  $\mu$ , respectively.

## IV. ADVERSARIAL WATER-FILLING OVER SPACE

We develop an AWF framework over space by augmenting (1) with linear power-shaping constraints. Consider the same variables  $(p, n, P, N, \beta_i, \sigma_i)$  and impose the linear constraint  $Ap \leq \hat{p}$ , where  $A \in \mathbb{R}_{\geq 0}^{S \times m}$  is a sparse nonnegative matrix encoding power limits across channels and  $\hat{p} \in \mathbb{R}^S$  denotes the corresponding constraint thresholds. The AWF problem over space is

$$\max_{p \geq 0, \mathbf{1}^\top p = P, Ap \leq \hat{p}} \min_{n \geq 0, \mathbf{1}^\top n = N} f(p, n), \quad (13)$$

where  $f(p, n)$  depends on the modulation model.

### A. Gaussian Water-filling

Under Gaussian water-filling, the achievable sum rate is

$$f(p, n) = \sum_{i=1}^m \log \left( 1 + \frac{\beta_i p_i}{\sigma_i + n_i} \right). \quad (14)$$

For fixed  $n$ , the objective is strongly concave in  $p$  over the polytope, while for fixed  $p$  with active components  $p_i > 0$ , the function  $f(p, n)$  is strongly convex in the interference variables  $n_i$ . Consequently, for Gaussian inputs, the AWF problem can be formulated as the following strongly convex–concave max–min game:

$$\max_{p \geq 0} \min_{n \geq 0} \sum_{i=1}^m \log \left( 1 + \frac{\beta_i p_i}{\sigma_i + n_i} \right), \quad (15)$$

subject to  $\mathbf{1}^\top p = P$ ,  $\mathbf{1}^\top n = N$ , and  $Ap \leq \hat{p}$ .

Problem (15) is more general than the formulation discussed in the previous section. In particular, the min–max problem in (3) can be recovered as the special case in which there are no additional spatial power constraints, i.e.,  $A = 0$  so that the constraint  $Ap \leq \hat{p}$  becomes inactive. Under these

additional linear constraints, the classical scalar water-level characterization no longer applies directly. Instead, the resulting water-filling solution becomes multi-dimensional, with the water levels coupled through the constraint  $Ap \leq \hat{p}$ .

Introduce dual variables  $\nu$  for the total transmit power constraint  $\mathbf{1}^\top p = P$ , and  $\theta \geq 0$  for the linear constraint  $Ap \leq \hat{p}$ . Let  $\mu$  denote the dual variable associated with the total interference power constraint  $\mathbf{1}^\top n = N$ . We denote by  $b \geq 0$  and  $c \geq 0$  the dual variables associated with the nonnegativity constraints  $p \geq 0$  and  $n \geq 0$ , respectively.

The Lagrangian is

$$\begin{aligned} \mathcal{L}(p, n, \nu, \mu, \theta, b, c) = & \sum_{i=1}^m \log \left( 1 + \frac{\beta_i p_i}{\sigma_i + n_i} \right) - \nu (\mathbf{1}^\top p - P) \\ & + \mu (N - \mathbf{1}^\top n) - \theta^\top (Ap - \hat{p}) \\ & + b^\top p - c^\top n. \end{aligned} \quad (16)$$

Since the objective induces a strongly convex–concave game and the feasible region is compact, the optimal solution is uniquely characterized by the KKT conditions.

**Theorem 2** (Adversarial Water-filling over Space). *Let  $(p^*, n^*)$  denote an optimal solution of (15). Then the optimal transmit power allocation satisfies*

$$p_i^* = \max \left( \frac{1}{\nu^* + (A^\top \theta^*)_i} - \frac{\sigma_i + n_i^*}{\beta_i}, 0 \right), \quad \forall i \quad (17)$$

where  $\nu^*$  and  $\theta^* \geq 0$  are the dual variables associated with the total power constraint  $\mathbf{1}^\top p = P$  and the linear constraint  $Ap \leq \hat{p}$ , respectively.

*Proof.* Fix  $n = n^*$ . The transmit power allocation problem

$$\max_{p \geq 0, \mathbf{1}^\top p = P, Ap \leq \hat{p}} \sum_{i=1}^m \log \left( 1 + \frac{\beta_i p_i}{\sigma_i + n_i^*} \right) \quad (18)$$

is a strictly concave maximization over a polytope and therefore admits a unique optimizer. The KKT conditions are necessary and sufficient.

From the Lagrangian (16), the stationarity condition with respect to  $p_i$  for each channel  $i$  gives

$$\frac{\beta_i}{\sigma_i + n_i^* + \beta_i p_i^*} = \nu^* + (A^\top \theta^*)_i - b_i^*. \quad (19)$$

If  $p_i^* > 0$ , then  $b_i^* = 0$ , yielding

$$p_i^* = \frac{1}{\nu^* + (A^\top \theta^*)_i} - \frac{\sigma_i + n_i^*}{\beta_i}. \quad (20)$$

If  $p_i^* = 0$ , the right-hand side is nonpositive. Combining both cases yields the water-filling expression.  $\square$

The linear constraints induce channel-dependent effective transmit power water levels for all active channel  $i$

$$\nu_{A_i}^* \triangleq \frac{1}{\nu^* + (A^\top \theta^*)_i}. \quad (21)$$

When  $\theta^* = 0$ , the global water level  $\nu^*$  is recovered, as shown in Fig. 3. The interference power subproblem

$$\min_{n \geq 0, \mathbf{1}^\top n = N} \sum_{i=1}^m \log \left( 1 + \frac{\beta_i p_i^*}{\sigma_i + n_i} \right) \quad (22)$$

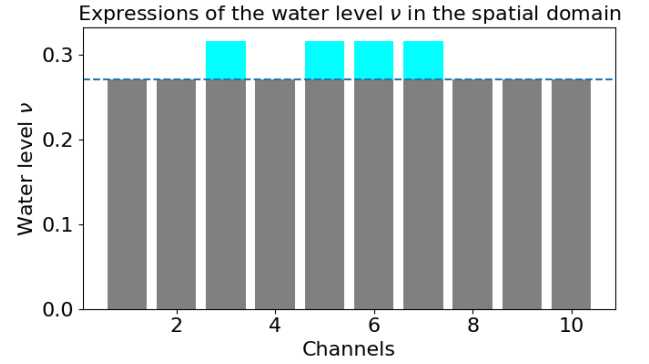


Fig. 3. Channel-wise effective water levels induced by the constraints. Gray bars represent the inverse effective levels  $1/\nu_{A_i}^*$ , while cyan segments correspond to the constraint-induced shift  $(A^\top \theta)_i$ . The dashed line denotes the global water level  $\nu^*$ .

is subject only to the simplex constraint. Consequently, the optimal interference allocation admits the inverse water-filling solution given in (5).

*PDHG on Gaussian Water-filling:* The adversarial water-filling problem over space in (15) forms a convex–concave minimax game. Such a saddle-point formulation can be efficiently solved using PDHG methods. Moreover, this primal–dual problem admits a water-filling interpretation. From this perspective, water levels arise as dual variables enforcing global power constraints, which in turn motivates the learned model developed later.

Consider the relaxation of a resource allocation problem

$$\min_x \sum_{i=1}^m f(x_i) + \mathbb{I}_C(x), \quad (23)$$

where  $C = \{x \in \mathbb{R}^m \mid \mathbf{1}^\top x = b, x \geq 0\}$ . Here  $\mathbb{I}_C(x)$  is an indicator function of  $C$ , taking value 0 if  $x \in C$  and  $+\infty$  otherwise. For the separable part  $f(x) = \sum_{i=1}^m f(x_i)$ , the proximal operator decomposes coordinate-wise for each channel  $i$  with proximal stepsize  $\tau > 0$  [42]:

$$[\text{prox}_{\tau f}(y)]_i = \arg \min_{x_i} \left\{ f(x_i) + \frac{1}{2\tau} (x_i - y_i)^2 \right\}. \quad (24)$$

Applying this framework to Gaussian water-filling, the power allocation subproblem for fixed interference  $n$  becomes

$$\min_p - \sum_{i=1}^m \log \left( 1 + \frac{\beta_i p_i}{\sigma_i + n_i} \right) + \mathbb{I}_{\tilde{C}}(p), \quad (25)$$

with  $\tilde{C} = \{p \mid p \geq 0, \mathbf{1}^\top p = P\}$ . The update can be interpreted as a separable proximal step for each channel followed by projection onto the simplex enforcing the total power constraint.

Under the PDHG framework [18], [19], the spectrum-domain formulation can be written as

$$\min_{p \geq 0} \max_{\nu} - \sum_{i=1}^m \log \left( 1 + \frac{\beta_i p_i}{\sigma_i + n_i} \right) + \nu \left( \sum_{i=1}^m p_i - P \right). \quad (26)$$

The corresponding PDHG updates take the form

$$\nu^{(k+1)} = \nu^{(k)} + \alpha \left( \sum_{i=1}^m p_i^{(k)} - P \right), \quad (27)$$

$$p_i^{(k+1)} = \text{prox}_{\tau f_i} \left( p_i^{(k)} - \tau \nu^{(k+1)} \right), \quad (28)$$

where  $f(p_i) = -\log \left( 1 + \frac{\beta_i p_i}{\sigma_i + n_i} \right)$ ,  $\forall i$ , and  $\alpha, \tau > 0$  denote the dual and primal stepsizes respectively. The dual update corresponds to the proximal step associated with the conjugate of the constraint indicator and reduces to an affine update in this setting. The dual variable  $\nu$  therefore parameterizes the global water level.

When additional linear constraints  $Ap \leq \hat{p}$  are present, the saddle problem introduces an additional dual variable  $\theta$ . The resulting primal update becomes

$$p_i^{(k+1)} = \text{prox}_{\tau f} \left( p_i^{(k)} - \tau (\nu^{(k+1)} + (A^\top \theta^{(k+1)})_i) \right), \quad \forall i \quad (29)$$

showing that the effective water level is determined jointly by the global dual variable  $\nu$  and the dual contribution  $A^\top \theta$  associated with the additional linear constraints.

### B. Mercury/water-filling

We now replace the Gaussian inputs with a general mutual-information objective. Let

$$f(p, n) = \sum_{i=1}^m I_i \left( \frac{\beta_i p_i}{\sigma_i + n_i} \right), \quad (30)$$

where  $I_i(\gamma)$  denotes the mutual information (in nats/use) of channel  $i$  at effective SINR  $\gamma$ . The AWF over space for channels under mercury/water-filling is

$$\max_{p \geq 0, \mathbf{1}^\top p = P, Ap \leq \hat{p}} \min_{n \geq 0, \mathbf{1}^\top n = N} \sum_{i=1}^m I_i \left( \frac{\beta_i p_i}{\sigma_i + n_i} \right). \quad (31)$$

Under standard regularity conditions on  $I(\cdot)$ , we characterize stationary points of the minimax problem through the KKT conditions. Introducing dual variables  $\nu$  for  $\mathbf{1}^\top p = P$  and  $\theta \geq 0$  for  $Ap \leq \hat{p}$ , Theorem 2 extends directly to imply that, for any  $i \in \{1, \dots, m\}$  with  $p_i^* > 0$ ,

$$\frac{\beta_i}{\sigma_i + n_i^*} I_i' \left( \frac{\beta_i p_i^*}{\sigma_i + n_i^*} \right) = \nu^* + (A^\top \theta^*)_i. \quad (32)$$

Since the feasible set for interference power is unchanged, for any  $i \in \{1, \dots, m\}$  with  $n_i^* > 0$ , we obtain

$$\frac{\beta_i p_i^*}{(\sigma_i + n_i^*)^2} I_i' \left( \frac{\beta_i p_i^*}{\sigma_i + n_i^*} \right) = -\mu^*. \quad (33)$$

where  $\mu^*$  enforces  $\mathbf{1}^\top n = N$ . Using the I-MMSE identity as in (12), the AWF over space for channels under mercury/water-filling admits the same water level interpretation as in the Gaussian case, with channel-dependent dual shifts induced by  $(A^\top \theta^*)_i$ .

*Mercury/water-filling and Proximal:* We now extend the proximal interpretation from Gaussian water-filling to mercury/water-filling. When the logarithmic objective is replaced by a general mutual-information function,

$$f(p_i) = -I_i \left( \frac{\beta_i p_i}{\sigma_i + n_i} \right), \quad \forall i \quad (34)$$

the problem remains separable across channels and continues to admit a primal–dual formulation.

However, the key difference lies in the form of the proximal operator. In the Gaussian case, the logarithmic objective leads to a rational derivative, yielding a quadratic optimality condition and hence a closed-form proximal update.

In contrast, under mercury/water-filling, the mutual information  $I(\gamma)$  induces a nonlinear dependence through the I-MMSE relationship. As a result, the proximal operator  $\text{prox}_{\tau f}(v)$  no longer admits a closed-form solution. Instead, each update requires solving a one-dimensional nonlinear equation of the form

$$p_i + \tau f'(p_i) = v, \quad \forall i, \quad (35)$$

where

$$f'(p_i) = -\frac{\beta_i}{\sigma_i + n_i} I_i' \left( \frac{\beta_i p_i}{\sigma_i + n_i} \right), \quad \forall i. \quad (36)$$

This leads to an implicit update that must be computed numerically for each channel. While each subproblem is one-dimensional, each primal–dual iteration still requires the solution of multiple per-channel nonlinear equations. This can become computationally burdensome in large-scale systems or in scenarios with heterogeneous input constellations, where the MMSE functions differ across channels. This loss of analytical tractability distinguishes mercury/water-filling from Gaussian water-filling and motivates incorporating an extragradient-style update within the foundation model in the next section.

## V. FOUNDATION MODEL ARCHITECTURE

The computational complexity of mercury/water-filling motivates replacing explicit proximal updates with learned primal–dual iterative dynamics. Unlike Gaussian water-filling, the associated updates generally do not admit closed-form solutions and instead require solving nonlinear implicit equations. This motivates a foundation model that learns the underlying AWF dynamics in a data-driven manner and can be interpreted as a learned generalization of primal–dual first-order methods.

The foundation model for AWF mirrors the KKT of adversarial water-filling: permutation-invariant encoding captures channel symmetry, graph neural message passing models sparse linear interactions induced by constraints, and learned primal–dual iterations approximate the coupled dynamics underlying water level coordination (cf. Fig. 4). Although primarily motivated by mercury/water-filling with discrete constellations, the framework ultimately applies to both Gaussian and mercury/water-filling settings, providing a unified and scalable approach. The Gaussian case is recovered as a special instance by choosing  $I_i(\gamma) = \log(1 + \gamma)$ ,  $\forall i$ .

### A. Architectural Motivation: Sets and Graphs

The water-filling problem exhibits several properties that guide the foundation model design. These include permutation invariance across channels, variable problem dimension, couplings induced by linear constraints, and low-dimensional global coordination through the KKT system. In particular, the channel parameters  $\{(\beta_i, \sigma_i)\}_{i=1}^m$  form an unordered set, and the problem is invariant to any permutation of channel indices. This motivates the use of permutation-invariant set representations.

To model global interactions among channels, we employ a Perceiver-style encoder<sup>1</sup>, in which a small set of learnable latent tokens first aggregates information from the input channel set and then exchanges information internally [37]. This fixed-size latent representation provides a compact summary of cross-channel competition and remains scalable as the number of channels varies. Linear constraints introduce couplings across channels. In particular, the constraint  $Ap \leq \hat{p}$  induces a natural bipartite graph between channel nodes and constraint nodes, which motivates a GNN-based module. Through message passing, constraint nodes aggregate and propagate information across related channels, approximating the coupling term  $A^\top \theta$  in the KKT conditions. Finally, the KKT system shows that global coordination is governed by a small number of positive optimal dual solution that act as water levels. We capture this structure through global latent representations that parameterize these water-level dynamics. By combining permutation-invariant set encoding with graph-based constraint propagation, this architecture incorporates the main features of AWF and supports generalization across different channel dimensions and constraint patterns.

### B. Problem Formulation

We consider the AWF problem over space under mercury/water-filling introduced in Section IV. Given channel parameters  $\{(\beta_i, \sigma_i)\}_{i=1}^m$ , total power budgets  $P, N$ , and linear constraints  $Ap \leq \hat{p}$ , the objective is

$$\max_{p \geq 0, \mathbf{1}^\top p = P, Ap \leq \hat{p}} \min_{n \geq 0, \mathbf{1}^\top n = N} \sum_{i=1}^m I_i \left( \frac{\beta_i p_i}{\sigma_i + n_i} \right). \quad (37)$$

The Gaussian case is recovered as a special instance by choosing  $I_i(\gamma) = \log(1 + \gamma)$ ,  $\forall i$ .

For discrete constellations, the derivative  $I'_i(\gamma)$  can be characterized via the I-MMSE identity [41], which provides a convenient basis for gradient-based optimization. The KKT conditions imply that for all active channels  $i$  with  $p_i > 0$ ,

$$I'_i(\gamma_i) \frac{\beta_i}{\sigma_i + n_i} = \nu + (A^\top \theta)_i, \quad (38)$$

where  $\nu$  and  $\theta$  are dual variables associated with the total budget and linear constraints and  $\gamma_i = \frac{\beta_i p_i}{\sigma_i + n_i}$ ,  $\forall i$ . Thus, coordination across channels is governed by a low-dimensional set of dual variables, with  $\nu$  acting as a global water level and  $A^\top \theta$  inducing channel-wise level shifts.

<sup>1</sup>The Perceiver, introduced in [37], is a transformer-style architecture that maps variable-size inputs into a small latent array through cross-attention, followed by latent self-attention. It is adopted here as an efficient mechanism for capturing global dependencies across channels.

### C. Foundation Model for AWF

We propose a foundation model for AWF that learns to emulate the underlying solution dynamics, including the associated water-level search, across varying channel dimensions, constraint patterns, and modulation formats. Rather than learning a direct channel-to-power mapping for a fixed problem size, the model learns an optimization problem that generalizes across scales and data distributions, thereby serving as a domain-specific foundation model for AWF problems.

1) *Distribution Token*: We sample  $L$  logarithmically spaced SINR points  $\{\gamma_j\}_{j=1}^L$  and construct a modulation-dependent feature vector

$$d = [I'(\gamma_1), \dots, I'(\gamma_L), I(\gamma_1), \dots, I(\gamma_L)], \quad (39)$$

which provides a compact numerical representation of the mutual-information curve associated with the modulation format. We refer to this feature vector as a distribution token, since it is treated as one input token by the learning model. Specifically, the entries  $I(\gamma_j)$  describe the value of the mutual information at representative SINR points, while  $I'(\gamma_j)$  captures the local variation of the curve. Thus,  $d$  encodes the modulation-dependent shape of the mutual-information function and is used as an input feature for the learning model. The values of  $I'(\gamma)$  are precomputed on a grid, and values at arbitrary  $\gamma_i^{(t)}$  are obtained by interpolation.

2) *Set Encoding and Global Water Level Representation*: Each channel is represented by

$$x_i = [\log \beta_i, \log \sigma_i, \phi(d_i)], \quad (40)$$

where  $\phi(\cdot)$  denotes a learned embedding of the distribution token. The unordered channel set  $\{x_i\}_{i=1}^m$  is processed by a permutation-invariant attention-based encoder

$$(h, Z) = \text{SetEncoder}(x), \quad (41)$$

which produces channel embeddings  $h_i$  together with a small set of learnable latent tokens  $Z$ .

The encoder uses a Perceiver-style architecture in which a small number of latent tokens  $Z$  first gather information from the channel set through cross-attention and then exchange information through latent self-attention. This latent bottleneck compresses a variable-size channel set into a fixed-size latent set  $Z$ , thereby capturing cross-channel competition while remaining scalable as the number of channels varies. The latent set  $Z$  summarizes set-level statistics and coordinates channel interactions. From an optimization perspective,  $Z$  plays a role analogous to the low-dimensional dual state in the KKT system and helps capture the effective water-level adjustment that equalizes marginal utility across channels.

3) *Constraint-Aware Message Passing via GNN*: Linear constraints introduce interactions between subsets of channels. We model these interactions using a GNN constructed from the constraint matrix  $A \in \mathbb{R}^{S \times m}$ . Specifically, we construct a bipartite graph with two types of nodes: channel nodes and constraint nodes. Each channel node represents one channel, or equivalently one optimization variable associated with that channel. Each constraint node represents one linear constraint, corresponding to one row of  $A$ . An edge is added between

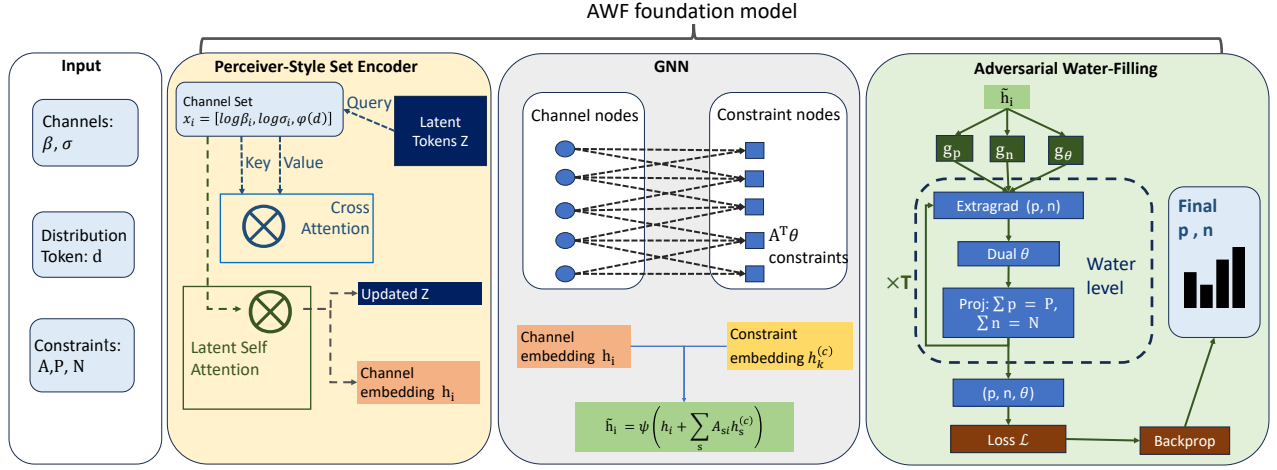


Fig. 4. Architecture of the foundation model for AWF. A Perceiver-style latent set encoder aggregates the channel set into channel embeddings and a global coordination state. GNN propagates constraint-induced interactions from the linear constraints. Learned primal–dual iterations perform iterative updates with budget projection. Training combines the gap, feasibility, and KKT losses. The model outputs channel-wise power allocations  $(p, n)$ .

channel node  $i$  and constraint node  $s$  whenever  $A_{si} \neq 0$ , indicating that channel  $i$  appears in constraint  $s$  with a nonzero coefficient. In this way, channels involved in the same linear constraint are connected through the corresponding constraint node, allowing the GNN to capture constraint-induced interactions among channels.

The GNN propagates information between channel nodes and constraint nodes through message passing. Message passing is performed in two stages. First, each constraint node aggregates information from its incident channels to form a constraint embedding

$$h_s^{(c)} = \psi \left( \sum_{i=1}^m A_{si} h_i \right), \quad (42)$$

where  $h_i$  denotes the channel embedding produced by the set encoder and  $\psi(\cdot)$  is a learnable transformation. This aggregation summarizes how the channel representations contribute to each constraint.

Second, the constraint embeddings are propagated back to the channel nodes,

$$\tilde{h}_i = \psi \left( h_i + \sum_{s=1}^S A_{si} h_s^{(c)} \right), \quad (43)$$

so that each channel receives feedback from the constraints in which it participates.

This GNN-based message passing mechanism enables constraint-induced interactions to propagate across channels while preserving the structure of  $A$ . From an optimization perspective, the feedback term approximates the coupling  $A^\top \theta$  in the KKT conditions, where  $\theta$  denotes the dual variables associated with the linear constraints. Consequently, the graph module provides a scalable learnable approximation to the constraint-induced channel-wise coupling and the resulting level shifts.

4) *Primal–Dual Iterations and Water-Level Search*: Initial allocations are predicted from the channel embeddings

$$p^{(0)} = P \cdot \text{softmax}(g_p(\tilde{h})), \quad n^{(0)} = N \cdot \text{softmax}(g_n(\tilde{h})). \quad (44)$$

Starting from these initial allocations, the model performs  $T$  learned primal–dual iterations that update the primal variables  $(p, n)$  together with the dual variable  $\theta$  associated with the linear constraints. Let  $\gamma_i = \frac{\beta_i p_i}{\sigma_i + n_i}$  denote the SINR of channel  $i$ . Using the I-MMSE identity, the gradient components of the saddle objective are given by

$$g_{p_i} = I'_i(\gamma_i) \frac{\beta_i}{\sigma_i + n_i} - (A^\top \theta)_i, \quad (45)$$

$$g_{n_i} = -I'_i(\gamma_i) \frac{\beta_i p_i}{(\sigma_i + n_i)^2}, \quad (46)$$

where  $g_{p_i}$  and  $g_{n_i}$  denote the gradient components with respect to  $p_i$  and  $n_i$ , respectively. The dual gradient is given by

$$g_\theta = Ap - \hat{p}. \quad (47)$$

Let  $z = (p, n, \theta)$  denote the stacked primal–dual variables and let  $G(z) = (g_p, -g_n, g_\theta)$  denote the saddle-gradient field. The model performs a projected extragradient update

$$z^{t+\frac{1}{2}} = \Pi_{\mathcal{X}}(z^t + D^t G(z^t)), \quad (48)$$

followed by the corrected step

$$z^{t+1} = \Pi_{\mathcal{X}} \left( z^{t+\frac{1}{2}} + D^t G(z^{t+\frac{1}{2}}) \right), \quad (49)$$

where  $D^t$  is a learned diagonal stepsize matrix predicted by the network, and  $\Pi_{\mathcal{X}}$  denotes projection onto  $\mathcal{X} = \Delta_P \times \Delta_N \times \mathbb{R}_{>0}^S$ .

The power budgets are enforced through simplex projection for both  $p$  and  $n$ , ensuring that the updated allocations satisfy  $\mathbf{1}^\top p = P$  and  $\mathbf{1}^\top n = N$ . These projections implicitly adjust the effective water level across channels, analogous to the water level search in water-filling problems. The dual variable  $\theta$  enforces the linear constraint  $Ap \leq \hat{p}$ , producing a differentiable primal–dual iteration that approximates the dynamics of the underlying minimax problem.

Through training across heterogeneous instances, the foundation model learns an update rule that rapidly drives the iterates toward near-stationary water levels under varying problem sizes, constraint types, and modulation distributions.

**Algorithm 1** Foundation Model for Adversarial Water-Filling

**Require:** Channel parameters  $\{(\beta_i, \sigma_i)\}_{i=1}^m$ , power budgets  $(P, N)$ , constraint matrix  $(A, \hat{p})$ , mutual-information tables  $(I, I')$ , iteration number  $T$

**Ensure:** Power allocations  $(p, n)$

- 1: Construct  $d_i = [I'_i(\gamma_j), I_i(\gamma_j)]_{j=1}^L$  for each channel
- 2: Form channel features  $x_i = [\log \beta_i, \log \sigma_i, \phi(d_i)]$
- 3: Compute channel embeddings and latent global state  $(h, Z) = \text{SetEncoder}(x)$
- 4: Compute constraint embeddings  $h_s^{(c)} = \psi(\sum_{i=1}^m A_{si} h_i)$
- 5: Update channel embeddings using the constraint GNN  $\tilde{h}_i = \psi\left(h_i + \sum_{s=1}^S A_{si} h_s^{(c)}\right)$
- 6: Initialize allocations  $p^{(0)} = P \cdot \text{softmax}(g_p(\tilde{h}))$ ,  $n^{(0)} = N \cdot \text{softmax}(g_n(\tilde{h}))$
- 7: Initialize dual variable  $\theta^{(0)} = 0$
- 8: **for**  $t = 0, 1, \dots, T - 1$  **do**
- 9:   Compute SINR  $\gamma_i^{(t)} = \frac{\beta_i p_i^{(t)}}{\sigma_i + n_i^{(t)}}$
- 10:   Evaluate  $I'(\gamma_i^{(t)})$
- 11:   Compute gradient components  $g_{p_i}^{(t)} = I'_i(\gamma_i^{(t)}) \frac{\beta_i}{\sigma_i + n_i^{(t)}} - (A^\top \theta^{(t)})_i$ ,  $g_{n_i}^{(t)} = -I'_i(\gamma_i^{(t)}) \frac{\beta_i p_i^{(t)}}{(\sigma_i + n_i^{(t)})^2}$ ,  $g_\theta^{(t)} = Ap^{(t)} - \hat{p}$
- 12:   Compute  $(\bar{p}, \bar{n}, \bar{\theta}) = \Pi_{\mathcal{X}}\left((p^{(t)}, n^{(t)}, \theta^{(t)}) + D^{(t)}(g_p^{(t)}, -g_n^{(t)}, g_\theta^{(t)})\right)$
- 13:   Compute corrected SINR  $\bar{\gamma}_i = \frac{\beta_i \bar{p}_i}{\sigma_i + \bar{n}_i}$
- 14:   Evaluate corrected gradient components using  $(\bar{p}, \bar{n}, \bar{\theta})$   
 $\bar{g}_{p_i} = I'_i(\bar{\gamma}_i) \frac{\beta_i}{\sigma_i + \bar{n}_i} - (A^\top \bar{\theta})_i$   
 $\bar{g}_{n_i} = -I'_i(\bar{\gamma}_i) \frac{\beta_i \bar{p}_i}{(\sigma_i + \bar{n}_i)^2}$ ,  $\bar{g}_\theta = A\bar{p} - \hat{p}$
- 15:   Update  $(p^{(t+1)}, n^{(t+1)}, \theta^{(t+1)}) = \Pi_{\mathcal{X}}\left((p^{(t)}, n^{(t)}, \theta^{(t)}) + D^{(t)}(\bar{g}_p, -\bar{g}_n, \bar{g}_\theta)\right)$
- 16:   Enforce constraints  $p^{(t+1)} \leftarrow \Pi_{\Delta_P}(p^{(t+1)})$ ,  $n^{(t+1)} \leftarrow \Pi_{\Delta_N}(n^{(t+1)})$
- 17:   Project the dual variable  $\theta^{(t+1)} \leftarrow \max(\theta^{(t+1)}, 0)$ .
- 18: **end for**
- 19: **return**  $(p^{(T)}, n^{(T)})$

*D. Training Objective*

We train on random AWF instances across varying channel dimensions, sparse constraint graphs, and modulation types. Define the normalized mutual-information objective

$$J(p, n) \triangleq \frac{1}{m_{\text{valid}}} \sum_{i=1}^m I_i\left(\frac{\beta_i p_i}{\sigma_i + n_i}\right). \quad (50)$$

The training objective is motivated by primal-dual optimality conditions for minimax problems and by PDHG-type algorithms [18], [19]. Rather than solving each instance to optimality, we measure how close the current iterate  $(p, n)$  is to a stationary point of the minimax problem using a tractable surrogate of the saddle residual based on a few projected ascent and descent steps. Specifically,

$$p^\uparrow \approx \text{Ascent}(p; n), \quad n^\downarrow \approx \text{Descent}(n; p), \quad (51)$$

where  $\text{Ascent}(\cdot)$  denotes a few projected updates that increase  $J(p, n)$  with respect to  $p$ , while  $\text{Descent}(\cdot)$  denotes a few projected updates that decrease  $J(p, n)$  with respect to  $n$ .

The resulting relative residual is

$$\mathcal{L}_{\text{gap}} = \frac{J(p^\uparrow, n) - J(p, n^\downarrow)}{|J(p, n)| + \epsilon}. \quad (52)$$

To promote feasibility with respect to the linear constraints, we introduce a smooth penalty

$$\mathcal{L}_{\text{ineq}} = \|\max(Ap - \hat{p}, 0)\|_2. \quad (53)$$

We further incorporate a stationarity regularizer derived from the KKT optimality conditions on active channels,

$$\mathcal{L}_{\text{kkt}} = \frac{1}{|\mathcal{A}_+|} \sum_{i \in \mathcal{A}_+} \left| I'_i(\gamma_i) \frac{\beta_i}{\sigma_i + n_i} - (A^\top \theta)_i - \nu \right|, \quad (54)$$

where  $\mathcal{A}_+ = \{i : p_i > \tau\}$  denotes the active channel set and  $\nu$  is the global water level associated with the simplex constraint, as characterized by (38).

The overall training objective combines saddle optimality, feasibility, and stationarity

$$\mathcal{L} = \mathcal{L}_{\text{gap}} + \lambda_{\text{ineq}} \mathcal{L}_{\text{ineq}} + \lambda_{\text{kkt}} \mathcal{L}_{\text{kkt}}. \quad (55)$$

The model is trained over heterogeneous AWF instances with varying channel dimensions, constraint graphs, and modulation distributions. As a result, the learned model generalizes not only across problem size and constraint types but also across distributional families, effectively learning the water level rather than a fixed-size regression mapping.

VI. THEORETICAL ANALYSIS

This section provides theoretical justification for the foundation model by analyzing the projected extragradient dynamics induced by the learned updates. The results characterize the behavior of the learned optimization dynamics, rather than that of a first-order algorithm.

Define the mutual-information objective

$$F(p, n) = \sum_{i=1}^m I_i(\gamma_i), \quad \text{s.t.} \quad \gamma_i = \frac{\beta_i p_i}{\sigma_i + n_i}. \quad (56)$$

We assume that  $\sigma_i > 0$  and  $\beta_i > 0$  for all  $i$ . The primal feasible sets are  $\Delta_P = \{p \in \mathbb{R}_{\geq 0}^m : \mathbf{1}^\top p = P\}$ ,  $\Delta_N = \{n \in \mathbb{R}_{> 0}^m : \mathbf{1}^\top n = N\}$ , together with the constraint  $Ap \leq \hat{p}$ ,  $A \in \mathbb{R}_{\geq 0}^{S \times m}$ . Introduce the partial Lagrangian

$$\mathcal{L}(p, n, \theta) = F(p, n) - \langle \theta, Ap - \hat{p} \rangle, \quad \theta \in \mathbb{R}_{\geq 0}^S. \quad (57)$$

For discrete constellations,  $I'_i(\gamma)$  can be related to the MMSE function through the I-MMSE identity. The gradients of the Lagrangian are

$$\nabla_{p_i} \mathcal{L}(p, n, \theta) = I'_i(\gamma_i) \frac{\beta_i}{\sigma_i + n_i} - (A^\top \theta)_i, \quad (58)$$

$$\nabla_{n_i} \mathcal{L}(p, n, \theta) = -I'_i(\gamma_i) \frac{\beta_i p_i}{(\sigma_i + n_i)^2}, \quad (59)$$

and

$$\nabla_\theta \mathcal{L}(p, n, \theta) = -(Ap - \hat{p}). \quad (60)$$

Let  $z = (p, n, \theta)$ , and define the product constraint set  $\mathcal{X} = \Delta_P \times \Delta_N \times \mathbb{R}_{\geq 0}^S$ . The saddle-gradient field is

$$G(z) = (\nabla_p \mathcal{L}(z), -\nabla_n \mathcal{L}(z), -\nabla_\theta \mathcal{L}(z)). \quad (61)$$

The learned model performs projected extragradient iterations of the form

$$z^{k+\frac{1}{2}} = \Pi_{\mathcal{X}}(z^k + D^k G(z^k)), \quad (62)$$

$$z^{k+1} = \Pi_{\mathcal{X}}\left(z^k + D^k G(z^{k+\frac{1}{2}})\right), \quad (63)$$

where  $D^k = \text{diag}(\alpha_p^k I_m, \alpha_n^k I_m, \alpha_\theta^k I_S)$  is a positive diagonal stepsize matrix predicted by the network and clamped to a bounded interval.

**Theorem 3** (Conditional KKT consistency). *Consider the projected extragradient updates in Lines 12–17 of Algorithm 1. Assume that  $I(\gamma)$  is continuously differentiable on  $[0, \Gamma_{\max}]$  and that  $\text{mmse}(\gamma)$  is bounded on this interval. Let  $z^* = (p^*, n^*, \theta^*) \in \mathcal{X}$  be a fixed point of the projected extragradient map (63), and suppose that it is also a fixed point of the underlying projected first-order step, namely,*

$$z^* = \Pi_{\mathcal{X}}(z^* + D^* G(z^*)) \quad (64)$$

for some diagonal matrix  $D^* = \text{diag}(\alpha_p^* I_m, \alpha_n^* I_m, \alpha_\theta^* I_S)$  with strictly positive diagonal entries. Then  $z^*$  satisfies the first-order KKT conditions of the AWF,

$$\nabla_p \mathcal{L}(p^*, n^*, \theta^*) \in N_{\Delta_P}(p^*), \quad (65)$$

$$-\nabla_n \mathcal{L}(p^*, n^*, \theta^*) \in N_{\Delta_N}(n^*), \quad (66)$$

together with  $Ap^* - \hat{p} \leq 0$ ,  $\theta^* \geq 0$ ,  $\theta^* \odot (Ap^* - \hat{p}) = 0$ .

*Proof.* At a fixed point, (64) and the optimality condition of Euclidean projection imply

$$z^* + D^* G(z^*) - z^* \in N_{\mathcal{X}}(z^*), \quad (67)$$

that is  $D^* G(z^*) \in N_{\mathcal{X}}(z^*)$ . Since  $D^*$  is block-diagonal and acts as multiplication by the positive scalars  $\alpha_p^*$ ,  $\alpha_n^*$ , and  $\alpha_\theta^*$  on the  $p$ -,  $n$ -, and  $\theta$ -blocks, respectively, the inclusion  $D^* G(z^*) \in N_{\mathcal{X}}(z^*)$  implies the corresponding blockwise inclusions after dividing by these positive scalars.

$$\nabla_p \mathcal{L}(p^*, n^*, \theta^*) \in N_{\Delta_P}(p^*), \quad (68)$$

$$-\nabla_n \mathcal{L}(p^*, n^*, \theta^*) \in N_{\Delta_N}(n^*), \quad (69)$$

and

$$-\nabla_\theta \mathcal{L}(p^*, n^*, \theta^*) \in N_{\mathbb{R}_{\geq 0}^S}(\theta^*). \quad (70)$$

Using (60), the last inclusion is equivalent to

$$Ap^* - \hat{p} \in N_{\mathbb{R}_{\geq 0}^S}(\theta^*), \quad (71)$$

which is precisely the complementarity system  $Ap^* - \hat{p} \leq 0$ ,  $\theta^* \geq 0$ ,  $\theta^* \odot (Ap^* - \hat{p}) = 0$ . Substituting the analytic gradients (58)–(60) gives the stated KKT conditions.  $\square$

**Theorem 4** (Foundation Model AWF). *Consider the simplex projection step in Line 15 of Algorithm 1. Let  $(p^*, n^*, \theta^*)$  be a KKT point of the AWF. Then for every active channel  $i \in \{1, \dots, m\}$  with  $p_i^* > 0$ , there exists a scalar  $\nu^*$  associated with the simplex constraint  $\mathbf{1}^\top p = P$  such that*

$$I'_i(\gamma_i^*) \frac{\beta_i}{\sigma_i + n_i^*} = \nu^* + (A^\top \theta^*)_i. \quad (72)$$

*Proof.* The KKT condition for the constrained maximization in  $p$  implies the existence of dual variable  $\nu^*$  for the simplex constraint  $\mathbf{1}^\top p = P$  and nonnegative  $b^*$  for  $p \geq 0$  such that  $\nabla_{p_i} \mathcal{L}(p^*, n^*, \theta^*) - \nu^* + b_i^* = 0$ . If  $p_i^* > 0$ , complementary slackness yields  $b_i^* = 0$ . Substituting (58) gives

$$I'_i(\gamma_i^*) \frac{\beta_i}{\sigma_i + n_i^*} = \nu^* + (A^\top \theta^*)_i, \quad (73)$$

which proves the claim for every active channel  $i \in \{1, \dots, m\}$  with  $p_i^* > 0$ .  $\square$

Under mercury/water-filling, the mutual-information objective is not guaranteed to be globally convex in  $n$ . Even when  $I_i(\cdot)$  is smooth, the mapping

$$n_i \mapsto I_i\left(\frac{\beta_i p_i}{\sigma_i + n_i}\right), \quad \forall i \quad (74)$$

can be nonconvex in  $n_i$ , depending on the constellation and the SNR regime. Accordingly, convex–concave guarantees for this minimax problem do not apply in general. The results below therefore establish only local convergence around regular stationary points.

**Assumption 1** (Local regularity). *For the projected extragradient iterations in Lines 12–17 of Algorithm 1, assume that there exists a neighborhood  $\mathcal{U}$  of a stationary point  $z^* = (p^*, n^*, \theta^*)$  such that:*

- (i)  $G$  is  $L_G$ -Lipschitz on  $\mathcal{U}$ ;
- (ii) the projected extragradient map is differentiable at  $z^*$  along the feasible tangent space;
- (iii) the Jacobian of the projected extragradient map at  $z^*$  has spectral radius strictly smaller than one.

Local convergence of extragradient-type methods around regular stationary points is consistent with standard results in variational inequality theory [18], [43].

**Theorem 5** (Local convergence and computational complexity). *Consider the learned projected extragradient iterations in Lines 12–17 of Algorithm 1. Under Assumption 1, there exist constants  $c \in (0, 1)$  and  $\delta > 0$  such that if  $\|z^0 - z^*\| \leq \delta$ , then the iterates generated by (62)–(63) remain in a neighborhood  $\mathcal{U}$  of  $z^*$  and satisfy*

$$\|z^{k+1} - z^*\| \leq c \|z^k - z^*\|. \quad (75)$$

*Hence the learned projected extragradient dynamics converge locally to  $z^*$  at a linear rate. In addition, one inference forward pass of the model has scaling*

$$\mathcal{O}(L_{\text{att}} m d^2 + Ed + T(m + E)), \quad (76)$$

*and inference memory complexity*

$$\mathcal{O}(md + E). \quad (77)$$

*Proof.* By Assumption 1, the projected extragradient map is differentiable in a neighborhood of  $z^*$ , and its Jacobian at  $z^*$  has spectral radius strictly smaller than one. Therefore the map is locally contractive after possibly shrinking the neighborhood. The contraction mapping theorem then implies linear convergence of the iterates to  $z^*$ .

For computational complexity, the encoder uses latent attention rather than full self-attention over all channels. Processing  $m$  channel tokens of dimension  $d$  across  $L_{\text{att}}$  layers costs  $\mathcal{O}(L_{\text{att}} m d^2)$  [37]. Constraint graph aggregation over the sparse matrix  $A$  requires  $\mathcal{O}(Ed)$  operations.

Each extragradient step evaluates elementwise gradients in  $\mathcal{O}(m)$  and sparse products of the form  $A p$  and  $A^\top \theta$  in  $\mathcal{O}(E)$ , yielding  $\mathcal{O}(m + E)$  per step. Summing over  $T$  steps gives the stated complexity bounds.  $\square$

Theorems 3 and 5 characterize the learned primal–dual dynamics of the foundation model. Fixed points satisfying the underlying projected first-order condition correspond to KKT points of the mercury/water-filling AWF over space. Although the objective may be nonconvex in  $n$ , the dynamics are locally stable around regular stationary points satisfying Assumption 1, with stepsize clamping helping maintain bounded updates in practice.

### VII. EXPERIMENTS

We evaluate the foundation model on the discrete-constellation AWF problem under varying channel dimensions and constraints.

#### A. Problem Setting

In the channels under mercury/water-filling, the mutual information depends on discrete constellations rather than the Gaussian logarithmic form. We use 16QAM and 64QAM during training, and obtain  $I'(\gamma) = \text{mmse}(\gamma)$  from precomputed interpolation tables on a logarithmically spaced SNR grid over approximately  $[-10, 30]$  dB. Channel gains and noise powers are sampled as  $\log \beta_i \sim \mathcal{N}(0, 0.6^2)$  and  $\log \sigma_i \sim \mathcal{N}(0, 0.25^2)$ . The per-channel transmit and interference budgets are sampled as  $\bar{P}, \bar{N} \sim \mathcal{U}(0.05, 0.5)$ , and the total budgets are set to  $P = m\bar{P}$  and  $N = m\bar{N}$ . Linear constraints are generated from sparse nonnegative matrices  $A \in \mathbb{R}^{K \times m}$ , where  $K = \max\{1, \lfloor \rho m \rfloor\}$  and  $\rho \sim \mathcal{U}(0.05, 0.30)$ . Each row of  $A$  is normalized to unit sum, and  $\hat{p}$  is generated by adding positive random slack to  $A p$  for a sampled feasible power allocation. Training uses  $m \in \{32, 64, 128, 256, 512\}$ , while evaluation additionally includes  $m = 16$  and the unseen large-scale case  $m = 1024$ . For modulation generalization, 256QAM is used only as a unseen held-out evaluation format.

The model is trained with Adam using learning rate  $10^{-4}$  and batch size 16, with  $T = 64$  unrolled projected extragradient updates. Training instances are generated online. Runtime is measured after warm-up over repeated runs on a single NVIDIA GeForce RTX 3050 GPU.

#### B. Baseline Algorithm

As a baseline we implement the Mirror-Prox method [43], a standard extragradient algorithm for the minimax problems and variational inequalities. The updates take the form

$$z^{k+\frac{1}{2}} = \Pi_{\mathcal{Z}} \left( z^k + \eta G(z^k) \right), \quad (78)$$

$$z^{k+1} = \Pi_{\mathcal{Z}} \left( z^k + \eta G(z^{k+\frac{1}{2}}) \right), \quad (79)$$

TABLE I  
SIZE GENERALIZATION COMPARISON BETWEEN THE FOUNDATION MODEL AND MIRROR-PROX.

$m$	Method	$J$	InEq	$\text{KKT}_p$	$\text{KKT}_n$	Time (ms)
16	Model	0.4988	$1.00 \times 10^{-5}$	$5.64 \times 10^{-2}$	$6.15 \times 10^{-2}$	1124.6
	Mirror-Prox	0.4995	$1.84 \times 10^{-3}$	$1.70 \times 10^{-3}$	$4.53 \times 10^{-2}$	19778.4
32	Model	0.5126	$3.93 \times 10^{-5}$	$4.46 \times 10^{-2}$	$6.82 \times 10^{-2}$	1127.8
	Mirror-Prox	0.5122	$8.49 \times 10^{-4}$	$1.56 \times 10^{-3}$	$4.94 \times 10^{-2}$	19617.0
64	Model	0.5440	$2.07 \times 10^{-4}$	$4.85 \times 10^{-2}$	$6.59 \times 10^{-2}$	1138.4
	Mirror-Prox	0.5439	$1.39 \times 10^{-3}$	$1.19 \times 10^{-3}$	$5.05 \times 10^{-2}$	19453.0
128	Model	0.4768	$8.57 \times 10^{-4}$	$7.29 \times 10^{-2}$	$6.96 \times 10^{-2}$	1159.4
	Mirror-Prox	0.4767	$2.31 \times 10^{-3}$	$1.84 \times 10^{-3}$	$5.58 \times 10^{-2}$	19759.2
256	Model	0.5277	$1.22 \times 10^{-3}$	$5.20 \times 10^{-2}$	$6.09 \times 10^{-2}$	1132.8
	Mirror-Prox	0.5283	$2.87 \times 10^{-3}$	$1.81 \times 10^{-3}$	$4.66 \times 10^{-2}$	19543.0
512	Model	0.5688	$1.89 \times 10^{-3}$	$7.08 \times 10^{-2}$	$6.35 \times 10^{-2}$	1200.0
	Mirror-Prox	0.5695	$3.83 \times 10^{-3}$	$1.76 \times 10^{-3}$	$4.85 \times 10^{-2}$	18950.8
1024	Model	0.5539	$1.37 \times 10^{-3}$	$2.64 \times 10^{-2}$	$5.87 \times 10^{-2}$	1183.1
	Mirror-Prox	0.5539	$2.45 \times 10^{-3}$	$1.59 \times 10^{-3}$	$4.68 \times 10^{-2}$	19483.1

where  $z = (p, n, \theta)$  denotes the primal–dual variables and  $G(z)$  is the saddle-gradient field defined in Section VI. The baseline uses analytic gradients with a fixed stepsize tuned for stable convergence.

#### C. Experiment I: Size Generalization

We first evaluate generalization across channel dimensions. For each dimension, new problem instances are generated by sampling channel parameters and constraint matrices from the same distributions as in training. Performance is measured using the normalized objective value  $J(p, n) = m_{\text{valid}}^{-1} \sum_{i=1}^m I_i(\gamma_i)$ , the average inequality violation of  $A p \leq \hat{p}$ , the stationarity residuals for both  $p$  and  $n$ , and the runtime. A single pre-trained model is frozen for all evaluation settings, and no instance-specific fine-tuning is performed.

Table I reports the results. Across all tested dimensions, the foundation model achieves objective values nearly identical to those obtained by the iterative Mirror-Prox baseline. The inequality violations remain small, showing that the learned primal–dual dynamics preserve feasibility across problem sizes. Mirror-Prox achieves smaller transmit-side KKT residuals because it is run for many iterative correction steps, whereas the foundation model trades stationarity accuracy for substantially lower latency. Nevertheless, the objective values remain close to those of Mirror-Prox, indicating that the learned finite-step dynamics provide fast approximate solutions rather than fully converged iterates. Importantly, the model remains stable when extrapolating to the unseen large-scale setting  $m = 1024$ , where it attains the same objective value as Mirror-Prox while using substantially less runtime.

A key advantage of the foundation model is computational efficiency. Fig. 5 reports the runtime statistics of the foundation model and the stable Mirror-Prox baseline over channel dimensions ranging from  $m = 16$  to  $m = 1024$ . For each dimension, both methods were executed repeatedly, and the mean runtime, standard deviation, and speedup ratio were recorded. Across all tested dimensions, the foundation model consistently outperforms Mirror-Prox, with runtime around one second, compared with tens of seconds for Mirror-Prox. This corresponds to a speedup of approximately  $16 \times - 18 \times$ , more than one order of magnitude.

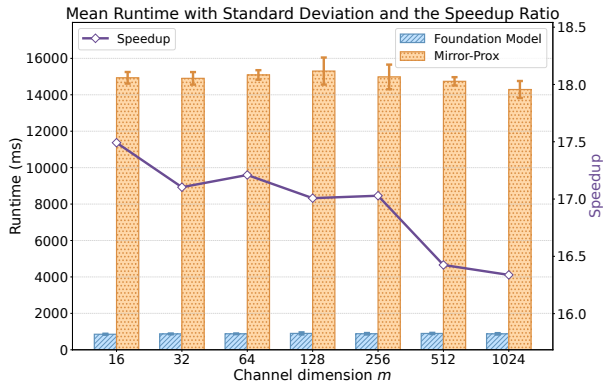


Fig. 5. Runtime comparison between the AWF foundation model and the stable Mirror-Prox baseline across different channel dimensions  $m$ . Bars represent the mean runtime over repeated runs, error bars denote one standard deviation, and the curve reports the corresponding speedup ratios.

TABLE II  
GENERALIZATION ACROSS MODULATION FORMATS AT  $m = 1024$ .

Modulation	Method	$J$	InEq	$KKT_p$	$KKT_n$	Time (ms)
16QAM	Model	0.5701	$1.34 \times 10^{-3}$	$3.36 \times 10^{-2}$	$5.28 \times 10^{-2}$	947.1
	Mirror-Prox	0.5711	$2.66 \times 10^{-3}$	$1.57 \times 10^{-3}$	$3.48 \times 10^{-2}$	14928.4
64QAM	Model	0.4299	$2.53 \times 10^{-3}$	$7.48 \times 10^{-2}$	$5.01 \times 10^{-2}$	939.8
	Mirror-Prox	0.4301	$3.93 \times 10^{-3}$	$2.27 \times 10^{-3}$	$4.17 \times 10^{-2}$	14360.7
Mixed	Model	0.5136	$1.85 \times 10^{-3}$	$7.00 \times 10^{-2}$	$5.75 \times 10^{-2}$	1153.5
	Mirror-Prox	0.5140	$3.03 \times 10^{-3}$	$1.88 \times 10^{-3}$	$4.90 \times 10^{-2}$	17155.3
256QAM	Model	0.5354	$1.05 \times 10^{-3}$	$1.64 \times 10^{-2}$	$1.04 \times 10^{-1}$	938.4
	Mirror-Prox	0.5349	$1.76 \times 10^{-3}$	$1.76 \times 10^{-3}$	$7.05 \times 10^{-2}$	14791.3

#### D. Experiment II: Modulation Generalization

We next evaluate generalization across modulation formats. Discrete constellations induce modulation-dependent curvature in the mutual-information function through the I-MMSE relationship, which changes the effective water-level dynamics. During training, each instance randomly uses either 16QAM or 64QAM modulation, encouraging the model to learn a shared update mechanism across constellation families. At evaluation time, we test the trained model on unseen instances with  $m = 1024$  under 16QAM, 64QAM, mixed 16QAM/64QAM settings, and a held-out unseen 256QAM setting. Table II summarizes the results. Across all modulation settings, the foundation model achieves objective values very close to those obtained by Mirror-Prox while maintaining substantially lower runtime. The held-out 256QAM results further indicate that the learned dynamics adapt to modulation-dependent MMSE curves rather than overfitting to the modulation formats used during training.

#### E. Experiment III: Constraint Generalization

We finally evaluate whether a single trained model generalizes to different linear constraint families. During training, constraint matrices are sampled from random sparse nonnegative patterns. At evaluation time, we test the in-distribution *sparse* random constraints as well as unseen constraint classes that are not explicitly observed during training: *group* constraints over disjoint channel subsets, *prefix* cumulative constraints, and *dense* correlated constraints with highly overlapping rows. Table III reports the results at the unseen large-scale setting  $m = 1024$ . Across all tested constraints, the

TABLE III  
GENERALIZATION ACROSS UNSEEN CONSTRAINTS AT  $m = 1024$ .

Constraint	Method	$J$	InEq	$KKT_p$	$KKT_n$	Time (ms)
Sparse	Model	0.6265	$1.49 \times 10^{-3}$	$2.95 \times 10^{-2}$	$5.21 \times 10^{-2}$	1014.0
	Mirror-Prox	0.6268	$2.64 \times 10^{-3}$	$2.31 \times 10^{-3}$	$4.54 \times 10^{-2}$	15723.4
Group	Model	0.4579	$1.15 \times 10^{-3}$	$9.67 \times 10^{-2}$	$4.67 \times 10^{-2}$	1056.6
	Mirror-Prox	0.4613	$4.09 \times 10^{-3}$	$2.02 \times 10^{-3}$	$3.97 \times 10^{-2}$	16935.1
Prefix	Model	0.4870	$3.62 \times 10^{-5}$	$2.19 \times 10^{-3}$	$4.54 \times 10^{-2}$	1074.1
	Mirror-Prox	0.4866	$1.55 \times 10^{-4}$	$8.07 \times 10^{-4}$	$3.82 \times 10^{-2}$	16895.5
Dense	Model	0.5819	$7.07 \times 10^{-6}$	$1.11 \times 10^{-3}$	$4.45 \times 10^{-2}$	1100.6
	Mirror-Prox	0.5814	$6.80 \times 10^{-6}$	$8.09 \times 10^{-4}$	$3.62 \times 10^{-2}$	16890.2

foundation model achieves objective values close to those of Mirror-Prox while maintaining low feasibility violation and a substantial runtime advantage. The primal-side KKT residual is smallest under prefix and dense constraints, whereas group constraints remain more challenging due to their disjoint structure. Overall, these results indicate that the AWF foundation model captures transferable primal-dual update patterns rather than overfitting to a single constraint generator.

## VIII. CONCLUSION

This paper has proposed the AWF as a unified framework for competitive spectrum and spatial resource allocation. While Gaussian adversarial water-filling gives rise to a strongly convex-concave game, practical discrete constellations lead to generally nonconvex mercury/water-filling formulations. To address this challenge, we have proposed a wireless foundation model that learns water level search dynamics across varying channel dimensions, constraints, and modulation distributions. The architecture integrates permutation-invariant channel representations, constraint-aware message passing, and global latent variables that reflect the optimal adversarial water level. Theoretical analysis characterized conditional KKT consistency and local convergence under regularity and contraction conditions. Experiments demonstrated empirical generalization across problem sizes, constraints, and modulation formats, while achieving significant runtime improvements over iterative baselines. Interesting problems for future work include extending this model to multi-agent wireless optimization problems, as well as incorporating additional system dynamics such as time-varying channels and network-level coordination in large-scale LEO deployments.

## REFERENCES

- [1] C.-X. Wang, X. You, X. Gao, X. Zhu, Z. Li, C. Zhang, H. Wang, Y. Huang, Y. Chen, H. Haas, J. S. Thompson, E. G. Larsson, M. D. Renzo, W. Tong, P. Zhu, X. Shen, H. V. Poor, and L. Hanzo, "On the road to 6G: Visions, requirements, key technologies, and testbeds," *IEEE Communications Surveys & Tutorials*, vol. 25, no. 2, pp. 905–974, 2023.
- [2] C.-F. Liu, M. Bennis, M. Debbah, and H. V. Poor, "Dynamic task offloading and resource allocation for ultra-reliable low-latency edge computing," *IEEE Transactions on Communications*, vol. 67, no. 6, pp. 4132–4150, 2019.
- [3] E. Habler, R. Bitton, D. Avraham, D. Mimran, E. Klevansky, O. Brodt, H. Lehmann, Y. Elovici, and A. Shabtai, "Adversarial machine learning threat analysis and remediation in open radio access network (O-RAN)," 2023. [Online]. Available: <https://arxiv.org/abs/2201.06093>
- [4] M. Polese, L. Bonati, S. D'Oro, S. Basagni, and T. Melodia, "CoO-RAN: Developing machine learning-based xApps for open RAN closed-loop control on programmable experimental platforms," *IEEE Transactions on Mobile Computing*, vol. 22, no. 10, pp. 5787–5800, Oct. 2023.

- [5] S. D'Oro, L. Bonati, M. Polese, and T. Melodia, "OrchestRAN: Network automation through orchestrated intelligence in the open RAN," in *Proceedings of the 2022 IEEE Conference on Computer Communications (INFOCOM)*, London, United Kingdom, 2022, pp. 270–279.
- [6] S. Chen, C. W. Tan, X. Zhai, and H. V. Poor, "OpenRANet: Neuralized spectrum access by joint subcarrier and power allocation with optimization-based deep learning," 2025. [Online]. Available: <https://arxiv.org/abs/2409.12964>
- [7] Federal Communications Commission, "Space exploration holdings, LLC request for deployment and operating authority for the spaceX Gen2 NGSO satellite system," Order and Authorization, DA 24-1193, 2024, accessed: 2026-05-13. [Online]. Available: <https://docs.fcc.gov/public/attachments/DA-24-1193A1.pdf>
- [8] Y. Li, Z. Ye, H. Zhang, J. Wang, J. Ma, and W. Tong, "Coded water-filling for multi-user interference cancellation," 2024. [Online]. Available: <https://arxiv.org/abs/2410.14136>
- [9] H. Al-Hraishawi, H. Chougrani, S. Kisseleff, E. Lagunas, and S. Chatzinotas, "A survey on nongeostationary satellite systems: The communication perspective," *IEEE Communications Surveys & Tutorials*, vol. 25, no. 1, pp. 101–132, 2023.
- [10] G. Giambene, S. Kota, and P. Pillai, "Satellite-5G integration: A network perspective," *IEEE Network*, vol. 32, no. 5, pp. 25–31, 2018.
- [11] S. Kassing, D. Bhattacharjee, A. B. Águas, J. E. Saethre, and A. Singla, "Exploring the "Internet from space" with Hypatia," in *Proceedings of the ACM Internet Measurement Conference*, New York, NY, USA, 2020, p. 214–229.
- [12] R. Smith, C. Freeberg, T. Machacek, and V. Ramaswamy, "An O-RAN approach to spectrum sharing between commercial 5G and government satellite systems," in *Proceedings of the 2021 IEEE Military Communications Conference (MILCOM)*, San Diego, CA, USA, Nov. 2021, pp. 739–744.
- [13] R. G. Gallager, *Information theory and reliable communication*. Springer, 1968, vol. 588.
- [14] A. Lozano, A. M. Tulino, and S. Verdú, "Optimum power allocation for parallel Gaussian channels with arbitrary input distributions," *IEEE Transactions on Information Theory*, vol. 52, no. 7, pp. 3033–3051, 2006.
- [15] D. P. Palomar and J. R. Fonollosa, "Practical algorithms for a family of waterfilling solutions," *IEEE Transactions on Signal Processing*, vol. 53, no. 2, pp. 686–695, 2005.
- [16] C. Xing, Y. Jing, S. Wang, S. Ma, and H. V. Poor, "New viewpoint and algorithms for water-filling solutions in wireless communications," *IEEE Transactions on Signal Processing*, vol. 68, pp. 1618–1634, 2020.
- [17] L. Zheng, Y.-W. P. Hong, C. W. Tan, C.-L. Hsieh, and C.-H. Lee, "Wireless max–min utility fairness with general monotonic constraints by Perron–Frobenius theory," *IEEE Transactions on Information Theory*, vol. 62, no. 12, pp. 7283–7298, 2016.
- [18] A. Chambolle and T. Pock, "A first-order primal-dual algorithm for convex problems with applications to imaging," *Journal of Mathematical Imaging and Vision*, vol. 40, no. 1, pp. 120–145, May 2011.
- [19] T. Goldstein, M. Li, X. Yuan, E. Esser, and R. Baraniuk, "Adaptive primal-dual hybrid gradient methods for saddle-point problems," 2015. [Online]. Available: <https://arxiv.org/abs/1305.0546>
- [20] B. Yang and M. Johansson, *Distributed Optimization and Games: A Tutorial Overview*. London: Springer London, 2010, pp. 109–148. [Online]. Available: [https://doi.org/10.1007/978-0-85729-033-5\\_4](https://doi.org/10.1007/978-0-85729-033-5_4)
- [21] H. Sun, X. Chen, Q. Shi, M. Hong, X. Fu, and N. D. Sidiropoulos, "Learning to optimize: Training deep neural networks for interference management," *IEEE Transactions on Signal Processing*, vol. 66, no. 20, p. 5438–5453, Oct. 2018.
- [22] J. Shao, J. Tong, Q. Wu, W. Guo, Z. Li, Z. Lin, and J. Zhang, "WirelessLLM: Empowering large language models towards wireless intelligence," 2024. [Online]. Available: <https://arxiv.org/abs/2405.17053>
- [23] X. Tong, C. W. Tan, and H. V. Poor, "Adversarial water-filling: Minimax resource allocation optimization with proximal decomposition in open ran," in *GLOBECOM 2025 - 2025 IEEE Global Communications Conference*, 2025, pp. 3933–3938.
- [24] T. M. Cover, *Elements of Information Theory*. John Wiley & Sons, 1999.
- [25] D. Tse and P. Viswanath, *Fundamentals of Wireless Communication*. Cambridge university press, 2005.
- [26] W. Yu, W. Rhee, S. Boyd, and J. Cioffi, "Iterative water-filling for Gaussian vector multiple-access channels," *IEEE Transactions on Information Theory*, vol. 50, no. 1, pp. 145–152, 2004.
- [27] W. Yu and R. Lui, "Dual methods for nonconvex spectrum optimization of multicarrier systems," *IEEE Transactions on communications*, vol. 54, no. 7, pp. 1310–1322, 2006.
- [28] A. Ghosh and S. Boyd, "Minimax and convex-concave games," 2003, EE392o Lecture course notes, Stanford University, Stanford, CA.
- [29] A. Garnaev, W. Trappe, and H. Vincent Poor, "Max-min resource allocation with application to anti-jamming," *IEEE Wireless Communications Letters*, vol. 15, pp. 1405–1409, 2026.
- [30] A. Garnaev, A. Petropulu, W. Trappe, and H. V. Poor, "An anti-jamming multiple access channel game using latency as metric," *IEEE Wireless Communications Letters*, vol. 11, no. 9, pp. 1800–1804, 2022.
- [31] H. Sun, W. Pu, X. Fu, T.-H. Chang, and M. Hong, "Learning to continuously optimize wireless resource in a dynamic environment: A bilevel optimization perspective," *IEEE Transactions on Signal Processing*, vol. 70, p. 1900–1917, 2022.
- [32] Y. S. Nasir and D. Guo, "Multi-agent deep reinforcement learning for dynamic power allocation in wireless networks," *IEEE Journal on Selected Areas in Communications*, vol. 37, no. 10, p. 2239–2250, Oct. 2019.
- [33] Y. Shen, Y. Shi, J. Zhang, and K. B. Letaief, "Graph neural networks for scalable radio resource management: Architecture design and theoretical analysis," *IEEE Journal on Selected Areas in Communications*, vol. 39, no. 1, pp. 101–115, 2021.
- [34] H. Yang, N. Cheng, R. Sun, W. Quan, R. Chai, K. Aldubaikhy, A. Alqasir, and X. Shen, "Knowledge-driven resource allocation for wireless networks: A WMMSE unrolled graph neural network approach," *IEEE Internet of Things Journal*, vol. 11, no. 10, pp. 18902–18916, 2024.
- [35] M. Zaheer, S. Kottur, S. Ravanbakhsh, B. Póczos, R. Salakhutdinov, and A. Smola, "Deep sets," 2018. [Online]. Available: <https://arxiv.org/abs/1703.06114>
- [36] J. Lee, Y. Lee, J. Kim, A. Kosiorek, S. Choi, and Y. W. Teh, "Set transformer: A framework for attention-based permutation-invariant neural networks," in *Proceedings of the 36th International Conference on Machine Learning*, ser. Proceedings of Machine Learning Research, K. Chaudhuri and R. Salakhutdinov, Eds., vol. 97, 09–15 Jun 2019, pp. 3744–3753.
- [37] A. Jaegle, F. Gimeno, A. Brock, O. Vinyals, A. Zisserman, and J. Carreira, "Perceiver: General perception with iterative attention," in *Proceedings of the 38th International Conference on Machine Learning*, ser. Proceedings of Machine Learning Research, M. Meila and T. Zhang, Eds., vol. 139, 18–24 Jul 2021, pp. 4651–4664.
- [38] L. Bonati, M. Polese, S. D'Oro, S. Basagni, and T. Melodia, "OpenRAN gym: AI/ML development, data collection, and testing for O-RAN on PAWR platforms," *Computer Networks*, vol. 220, p. 109502, 2023.
- [39] S. Boyd and L. Vandenberghe, *Convex Optimization*. Cambridge University Press, 2004.
- [40] C. W. Tan, S. Friedland, and S. H. Low, "Spectrum management in multiuser cognitive wireless networks: Optimality and algorithm," *IEEE Journal on Selected Areas in Communications*, vol. 29, no. 2, pp. 421–430, 2011.
- [41] D. Guo, S. Shamai, and S. Verdú, "Mutual information and minimum mean-square error in Gaussian channels," *IEEE Transactions on Information Theory*, vol. 51, no. 4, pp. 1261–1282, 2005.
- [42] N. Parikh and S. Boyd, "Proximal algorithms," *Foundations and Trends® in Optimization*, vol. 1, no. 3, pp. 127–239, 2014.
- [43] A. Nemirovski, "Prox-method with rate of convergence  $O(1/t)$  for variational inequalities with Lipschitz continuous monotone operators and smooth convex-concave saddle point problems," *SIAM Journal on Optimization*, vol. 15, no. 1, pp. 229–251, 2004.